Determination of the electron affinity of iodine

J. Phys. B: At. Mol. Opt. Phys. **25** (1992) 1773–1783. Printed in the UK

Determination of the electron affinity of iodine

D Hanstorp and M Gustafsson

Department of Physics, Chalmers University of Technology and University of Göteborg, S-41296 Göteborg, Sweden

Received 9 December 1991

Abstract. The electron affinity of atomic iodine has been determined to be 3.059 038(10) eV. A beam of negatively charged iodine ions was merged collinearly with a laser beam. The onset of the photodetachment process was observed when the wavelength of the laser was scanned, and the result was fitted according to the Wigner law in order to determine the photodetachment threshold. The wavelength was calibrated by simultaneously recording the atomic spectra of lead and manganese as well as the fringes from a Fabry-Pérot reference etalon.

1. Introduction

The properties of negative ions differ considerably from those of neutral atoms. The outermost electron in a negative ion is effectively shielded from the electrostatic attraction of the nucleus by the other electrons, resulting in a relatively small binding energy. As a consequence, excitation to the continuum is possible by the use of commercially available dye lasers, even without any frequency doubling. This is in sharp contrast to neutral atoms, for which wavelengths in the UV or VUV region are normally necessary in order to reach the continuum. Another unique property of the negative ions is the limited number of excited states. In most negative ions there is only one bound state. Therefore, the electron affinity, defined as the difference in energy between the ground state and the continuum threshold, is usually the only optical transition which can be determined with high resolution. Although many states lying above the continuum threshold have been observed in negative ions they are generally very short lived and their energy can thus not be determined with high accuracy.

The most general laser method for determining the electron affinity of an element is laser photodetached electron spectrometry (LPES). This technique has been applied to a majority of the elements that can form stable or metastable negative ions (Hotop and Lineberger 1985). By this method, a fixed-frequency laser with a photon energy larger than the electron affinity radiates the negative ions. The extra electron can be detached, and its kinetic energy is measured with an electrostatic energy analyser. The best resolution obtained with this method is of the order of a few meV (Breyer *et al* 1978, Hotop and Lineberger 1985).

In order to improve accuracy, the laser photodetachment threshold (LPT) method, by which the onset of the photodetachment process is studied, can be used. Negative ions are illuminated with light from a tunable laser, and the threshold wavelength for the process

$$X^- + h\nu \rightarrow X + e^- \qquad (1)$$

0953-4075/92/081773+11$04.50

is determined. Several experimental techniques have been applied, in which either an increase in the final products of the process, i.e. neutral atoms or free electrons, or a decrease in the number of negative ions can be observed. For example, the decrease of the number of negative ions stored in an ion trap has been observed in order to determine the electron affinity of selenium and sulphur (Mansour *et al* 1988). However, negative ions formed into a beam is the most commonly used experimental method. The electron affinity of oxygen, which so far is the most accurately measured electron affinity, has been determined with this technique (Neumark *et al* 1985). In that experiment, both the neutral atoms and the emitted electrons were used for the detection. The main limitation of the laser photodetachment threshold method is the lack of high intensity tunable lasers that work in the required wavelength region which is normally in the infrared part of the spectrum. Only 18 elements have their photodetachment thresholds at wavelengths below 1000 nm.

The negative halogen ions form an especially interesting group of negative ions which has been studied both experimentally (Blondel *et al* 1989a, b) and theoretically (Crance 1987, 1988, Radojević *et al* 1987). Their ground state configuration is the same as the ground state of a noble gas atom. This implies that the photodetachment process is similar to the photoionization process for the noble gases which are the most commonly studied elements in photoionization spectroscopy. However, there is a major difference in the potential felt by the electrons being excited in the two systems. In a noble gas atom the electrons are bound by an ordinary Coulomb potential, while the outermost electron in a negative ion feels a short range potential. Since the short range potential makes the theoretically interesting electron correlation effect more pronounced, the negative ions are suitable for testing theoretical models. Since the ground state configuration is a closed shell ($np^6\ ^1S_0$), the negative halogen ions show neither fine nor hyperfine structure. In addition, since there is only one bound state in a halogen ion, the lower state in an excitation process is well defined.

Negative iodine ions have been investigated in several experimental and theoretical works, with emphasis on continuum excitation (Amusia *et al* 1990, Radojević *et al* 1987) and multiphoton processes (L'Huillier and Wendin 1988, Blondel *et al* 1987). The binding energy of iodine is 3 eV, therefore a continuum excitation can be performed with only two photons from the strongest line of an argon ion laser ($\lambda = 514$ nm) or three photons from the fundamental line of a Nd:YAG laser ($\lambda = 1064$ nm), and iodine was also the first negative ion for which a multiphoton process was observed (Hall *et al* 1965). So far, the most accurate value, 3.0591 (1) eV, of the electron affinity of iodine has been obtained by Webster *et al* (1983) using an optogalvanic technique. In this paper we report on a measurement of the electron affinity of iodine by detecting the production of the neutral iodine atoms produced in a field-free region using collinear laser and ion beams. The accuracy of the electron affinity is improved by one order of magnitude in comparison with the experiment by Webster *et al*.

2. Experimental set-up

The experiment is performed with an ion beam apparatus in which light from a laser interacts collinearly with negative ions. Fast neutral atoms produced by the photodetachment process are detected, and the rate of this production is monitored as a function of the laser wavelength. A schematic diagram of the experimental set-up is shown in figure 1.

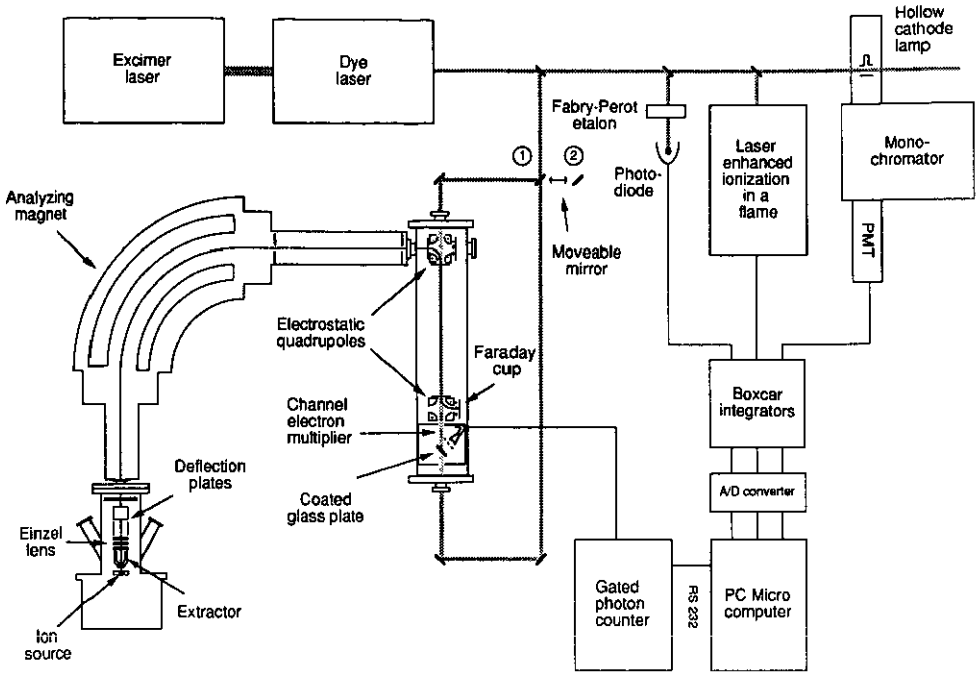

Figure 1. Schematic diagram of the apparatus.

As a more detailed description of the ion beam apparatus is to be published elsewhere (Hanstorp 1991), only a brief presentation is given here. Negative iodine ions are formed from I_2 on a hot surface (LaB_6). The ions are accelerated to 3 keV and mass analysed in a 50 cm sector magnet. The ions are then deflected 90° twice in two electrostatic quadrupoles placed 50 cm apart. The number of ions that has passed through the two quadrupoles is monitored with a Faraday cup placed after the second quadrupole. The I^- ion current measured at this point is typically 6 nA. The ions are illuminated with laser light in the region between the two quadrupoles, and the light can be directed either parallel or antiparallel with respect to the ion beam direction. Fast neutral atoms produced by the photodetachment process are not affected by the second quadrupole. Instead, they impinge on a glass plate placed behind the second quadrupole. Secondary electrons produced by the neutral atoms are collected with a channel electron multiplier (CEM) operated in a pulse counting mode. The CEM is carefully shielded, both mechanically and electrically, in order to prevent stray electrons from reaching the detector. This is described in more detail in Hanstorp (1992).

The signal from a single laser pulse recorded with a 250 MHz sampling oscilloscope is shown in the upper curve in figure 2. The laser is triggered at t equals zero, and the signal at this point is due to the photoelectric effect induced in the glass plate by the laser light. The signal from the neutral atoms arrives between $t = 1.8$ μs and $t = 9.3$ μs. This time interval, which is shown as the lower curve in figure 2, corresponds to the travelling time for the neutral atoms from the interaction region between the quadrupoles to the glass plate. Negative ions in the interaction region can also be neutralized due to collision with residual gas, resulting in a background signal. A second counting period from $t = 22$ μs to $t = 29.5$ μs is therefore used for a background subtraction,

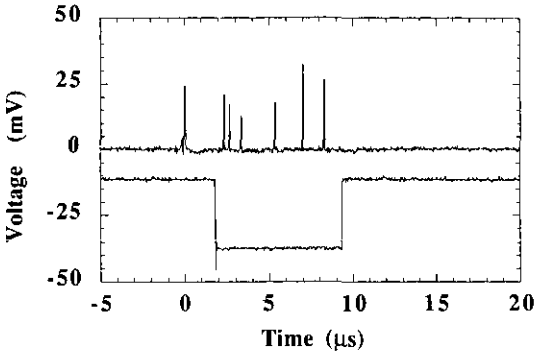

Figure 2. Oscilloscope trace of the photodetachment signal from a single laser pulse. The upper curve shows the signal from the channel electron multiplier while the lower curve shows the time when the photon counter, used to record the neutral particle, is enabled.

although this signal is virtually zero due to the low pressure in the interaction region ($\approx 10^{-9}$ mbar).

The laser system used in this experiment is an excimer pumped dye laser (Lambda Physik: LPX 210i and Fl 3002 E). A pulse energy of typically 8 mJ was obtained from the dye laser, using the dye DPS (Lambda Physik LC 4090), when it was pumped with 120 mJ from the excimer laser. The dye laser is equipped with an intracavity etalon (free spectral range 30 GHz) resulting in an effective frequency width of 1.2 GHz. The laser can be scanned continuously over a 1.1 nm wavelength region.

Much of the experimental set-up is used to calibrate the laser wavelength. Two atomic absorption experiments and one Fabry-Pérot reference etalon are required in order to make an absolute wavelength calibration.

An atomic line of lead is observed with laser induced fluorescence in a hollow cathode lamp. Lead atoms are excited from a metastable state, and the fluorescence back to the ground state is observed. A monochromator filters the fluorescence which then is detected with a photomultiplier tube.

Three atomic absorption lines of manganese are observed using laser-enhanced ionization (LEI) in an acetylene-air flame. With this technique, atoms being excited by the laser light are ionized by collisions with surrounding molecules in the flame. The electrons produced are collected by a voltage applied across the interaction region. This very sensitive method has mainly been used for trace element analysis, and the system used in this experiment is described in Axner *et al* (1984).

An 18 GHz Fabry-Pérot reference etalon is used as a frequency marker. The etalon is mounted in a large metal block which is placed inside a thermally insulated box, all in order to reduce the temperature drift during the experiment.

A PC microcomputer is used for collecting, storing and analysing the data. The pulses from the CEM are counted with a gated photon counter (Stanford Research System SRS 400) which is controlled by the microcomputer via an RS 232 interface. The three signals used in the wavelength calibration are all measured by means of boxcar integrators and fed into the microcomputer through an AD converter interface.

3. Experimental spectrum

Figure 3 shows one complete scan of a spectrum from the experiment, where the four

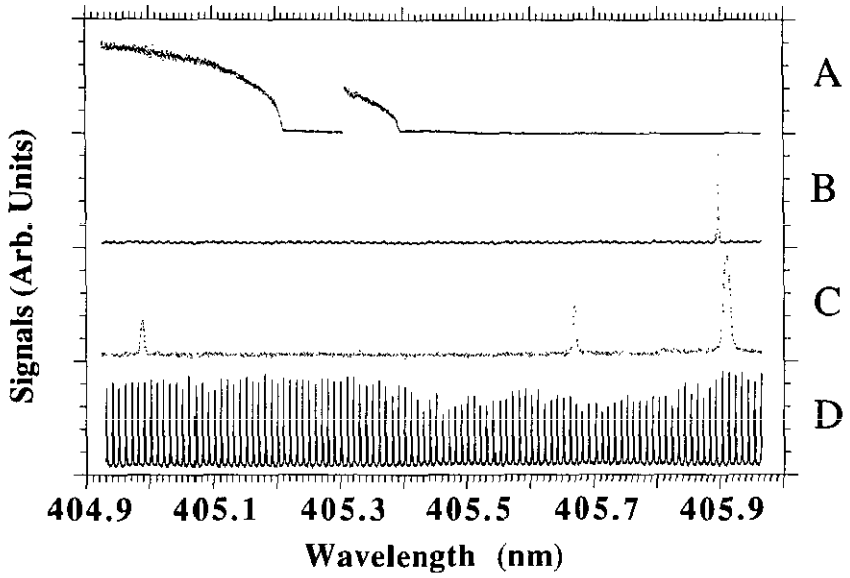

Figure 3. A complete recording of a spectrum. The signals shown are: A, photodetachment of I^-; B, laser induced fluorescence of lead in a hollow cathode lamp; C, laser enhanced ionization of manganese in an acetylene-air flame; and D, Fabry-Pérot fringes.

curves are: A, the relative photodetachment cross section of I^-; B, fluorescence from lead in a hollow-cathode lamp; C, laser-enhanced ionization of manganese in an acetylene-air flame; and D, Fabry-Pérot fringes.

The photodetachment threshold wavelength is strongly Doppler shifted due to the high velocity of the ions (7×10^4 m s^{-1}, corresponding to a shift of 0.1 nm), and the sign of the shift depends on the relative direction of the ion and laser beams. The Doppler shift can, however, be eliminated by performing two independent measurements of the threshold with the laser and ion beams parallel and antiparallel, respectively. In figure 3, the wavelength has been scanned from shorter to longer wavelengths. The laser and ion beams were made parallel at the beginning of the scan by placing the movable mirror, shown in figure 1, in position 1. At $\lambda = 405.3$ nm, when the laser had scanned through the photodetachment threshold, the direction of the laser beam was reversed by moving the movable mirror to position 2. At this point, the laser has not yet passed the photodetachment threshold for antiparallel ion and laser beams. The photodetachment thresholds with the laser and ion beams in both parallel and antiparallel geometries can then be measured in the same scan, as can be seen in curve A of figure 3.

The laser wavelength was scanned from 404.9 to 406.0 nm in steps of 0.000 27 nm. At each wavelength the signal from 30 laser pulses was averaged. In order to avoid saturation of the photodetachment signal, the pulse energy of the laser light in the interaction volume was attenuated to only 50 μJ.

4. Threshold determination

In order to determine the photodetachment threshold, the shape of the threshold must be investigated. According to the Wigner law (Wigner 1948), the photodetachment

cross section σ near the threshold varies as

$$\begin{aligned} \sigma &= c(E-E_0)^{l+1/2} \qquad E \geqslant E_0 \\ \sigma &= 0 \qquad\qquad\qquad\quad E < E_0 \end{aligned} \tag{2}$$

where c is a constant, E the energy of the light, E_0 the threshold energy and l is the angular momentum of the outgoing electron. In many cases the region where the threshold law is valid is several meV wide (Lineberger and Woodward 1970), while in some special cases it is valid for a considerably smaller energy interval (Peterson *et al* 1985). The excited electron in the negative iodine ion is initially a p electron, so the outgoing electron is either an s or a d electron. In the vicinity of the threshold a centrifugal barrier prevents the outgoing electron from being a d electron and, hence, there is a pure s-wave detachment. The threshold energy E_0 can then be determined by fitting the datum points to the Wigner law with l equals zero.

However, the shape of the photodetachment threshold is complicated by the hyperfine structure. The only stable isotope of iodine (^{127}I) has a nuclear spin of $\frac{5}{2}$. The ground state of the iodine atom, which has a configuration of $5p^5\,{}^2P_{3/2}$, is split into four hyperfine structure levels, with F values of 1, 2, 3 and 4, where $F=1$ has the lowest energy. The $^2P_{1/2}$ fine-structure component is located more than 1 eV above the ground state and cannot be populated in this experiment. The ground state configuration of the negative iodine ion, $5p^6\,{}^1S_0$, shows, as stated previously, neither fine nor hyperfine structure. With one initial state and four possible final states there are four independent photodetachment channels. The difference in threshold energy for the four channels corresponds to the hyperfine structure separations of the ground state of the iodine atom which have been determined by Fuller (1976). Since the electron affinity is defined as the energy difference between the ground state of the atom and the ground state of the negative ion, it is the threshold energy for the transition to the $F=1$ state which corresponds to the electron affinity. However, the photodetachment signal recorded in the experiment is the superposition of the four excitation channels. It is therefore necessary to treat all four photodetachment channels in the same fitting procedure.

As stated in Blondel *et al* (1989a), it can be shown that the relative cross section for the different channels is proportional to the multiplicity of the final state in the neutral atom, i.e. proportional to $2F+1$. This simple intensity relation is valid only when the initial state is non-degenerate. Therefore the iodine photodetachment threshold can be fitted to the function

$$\sigma = c \sum_{F=1}^{4} (2F+1)[E-(E_0+E_{\mathrm{hfs}}^F)]^{1/2} \tag{3}$$

where F is the hyperfine structure component of the neutral iodine atom, E_{hfs}^F its hyperfine-structure energy (Fuller 1976), E_0 the threshold energy for the $F=1$ component (i.e. the electron affinity) and c is a constant which depends on the specific excitation. Although this function is rather complex, there are only two parameters to be determined in a fit, namely c and E_0. All other parameters are known.

Before the experimental data can be fitted to equation (3), there is another effect which has to be considered. The emission from the laser contains, besides the laser line, a broad band emission of light, known as amplified spontaneous emission (ASE), with its centre frequency at the centre of the dye profile. Unfortunately, the amplified spontaneous emission is enhanced by introducing the intracavity etalon in the laser

resonator. If this emission of light is more energetic than the laser line, the photodetachment process might be induced even if the energy of the laser line is less than the electron affinity. However, since the amplified spontaneous emission is a broad-band radiation, the photodetachment signal induced by the emission changes slowly when the wavelength of the laser is tuned. We can therefore approximate this effect with a linear function, which is added to equation (3). The threshold can now be determined by fitting the data points in the vicinity of the threshold to the function

$$\sigma = c \sum_{F=1}^{4} (2F+1)[E-(E_0+E_{\mathrm{hfs}}^F)]^{1/2} + a(E-E_0) + b. \tag{4}$$

Figure 4 shows the relative cross section for the photodetachment from iodine when the laser and ion beams are parallel. The points are the experimental data and the full curve is the curve fitted to the theory as described above. The signal below the threshold, i.e. the signal from the amplified spontaneous emission, is almost constant. The hyperfine structure in the iodine atom can be seen as the small humps in the fitted function.

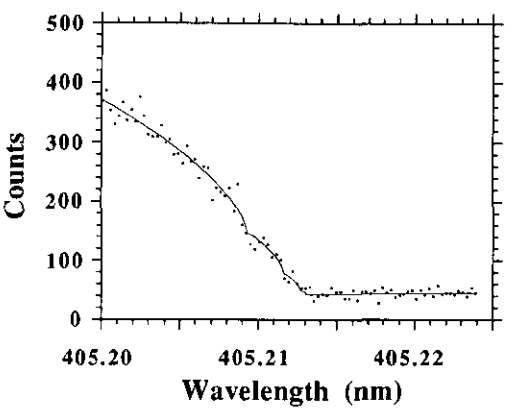

Figure 4. The relative photodetachment cross section in the vicinity of the threshold recorded with parallel laser and ion beams. The points are the experimental data and the full curve is a least-squares fit to the theoretical function given in equation (4).

As mentioned previously, the photodetachment threshold has been determined with the laser and ion beams both parallel and antiparallel. Each measured photodetachment threshold, E_{Th}, is then Doppler shifted according to the formula

$$E_{\mathrm{Th}}^{\mathrm{p,a}} = E_{\mathrm{EA}}(1 \pm v/c)[1-(v/c)^2]^{-1/2} \tag{5}$$

where E_{EA} is the unshifted threshold, p and a designate parallel or antiparallel laser and ion beams and v is the ion beam velocity. The unshifted threshold energy can now be obtained by taking the geometrical mean of the two measured quantities:

$$\begin{aligned}(E_{\mathrm{Th}}^{\mathrm{p}} E_{\mathrm{Th}}^{\mathrm{a}})^{1/2} &= \{E_{\mathrm{EA}}(1+v/c)[1-(v/c)^2]^{-1/2} E_{\mathrm{EA}}(1-v/c)[1-(v/c)^2]^{-1/2}\}^{1/2} \\ &= (E_{\mathrm{EA}} E_{\mathrm{EA}})^{1/2} = E_{\mathrm{EA}}. \end{aligned} \tag{6}$$

The quantity v/c cancels to all orders and the velocity of the ion beam can be left undetermined.

5. Wavelength calibration

As mentioned previously, the wavelength calibration in this experiment consisted of three parts.

Laser induced fluorescence of lead in a hollow cathode lamp was used for an absolute wavelength calibration. Hollow cathode lamps are well suited for use as wavelength standards, as shown by Crosswhite (1975). The upper curve in figure 5 shows the fluorescence spectrum for lead recorded around 405.9 nm. The structure of the line is due to the isotope shift, where the two largest peaks correspond to ^{208}Pb and ^{206}Pb, respectively. Wood and Andrew (1968) have measured the lead spectra using isotopically pure ^{208}Pb, where the vacuum wavelength of the $6s^26p^2(^3P_2) \rightarrow 6s^26p7s(^3P_1)$ transition was determined to be 405.895 28 (3) nm. The position of the main peak, determined with a least-squares fit to a Lorentzian curve, could therefore be used as a wavelength reference. The individual peaks have widths of approximately 1.2 GHz, which corresponds to the width of the laser.

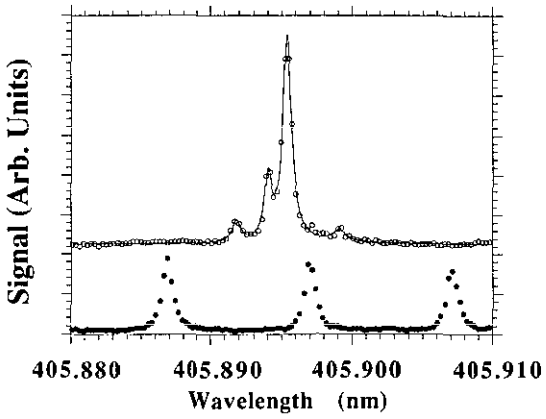

Figure 5. Upper curve: laser induced fluorescence from lead in a hollow cathode lamp. The circles are the data points and the solid line is a fitted function. Lower curve: Fabry-Pérot fringes.

The second step in the calibration procedure was to linearize the wavelength scale by means of the Fabry-Pérot fringes. Each transmission peak is fitted to a Lorentzian, and the centre frequencies of the fringes are then fitted to a polynomial function. The amplitude variation of the Fabry-Pérot fringes, as can be seen in figure 3, is a consequence of the limited number of samples per fringe (see the lower curve in figure 5).

Finally, the free spectral range (FSR) of the Fabry-Pérot etalon was determined. This can be done when at least two well known reference wavelengths are within the laser scan, and indeed three manganese lines were found in the desired wavelength region (Reader and Corliss 1980, Catalán *et al* 1964). Unfortunately, these manganese lines were too weak to be observed in a hollow cathode lamp, therefore we had to use the more sensitive method of laser-enhanced ionization (LEI) in a flame. The disadvantage of this technique is that the experiments are done at high temperature and pressure, giving rise to pressure broadening of the absorption lines, resulting in linewidths of 15 GHz. An even more serious problem is that the lines are slightly red shifted due to collisions in the flame. According to Wagenaar and de Galan (1973) this shift is of

Table 1. Manganese reference wavelengths.

Transition	λ_{air} (nm)	λ_{vacuum} (nm)
$3d^64s\ ^6D_{5/2} \rightarrow 3d^64p\ ^6D_{3/2}$	404.8747	404.9887
$3d^64s\ ^6D_{7/2} \rightarrow 3d^64p\ ^6D_{7/2}$	405.5548	405.6690
$3d^54s4p\ ^6P_{3/2} \rightarrow 3d^54s5s\ ^6S_{5/2}$	405.7954	405.9096

the order of 20% of the linewidth, which in this case becomes approximately 3 GHz. Since we have three manganese lines, we have two independent wavelength separations which can both be used to determine the FSR of the Fabry-Pérot etalon. The two values of the FSR differ by only 4 MHz, and we can conclude that the three different lines are shifted equally (within the statistical uncertainty of the measurement). There are two compilations of the wavelengths in the manganese spectrum (Reader and Corliss 1980, Catalán *et al* 1964) which present almost the same wavelengths, and we have chosen to use the results of Catalán *et al* for two reasons. First, they are based on the most recent measurement. Second, all lines in the work by Catalán *et al* were used to calculate the energy level diagram of manganese, for which every energy level is calculated by using all transitions to that level. Thereafter, the transition wavelengths calculated by means of the energy level diagram are compared with the measured values. For the three transitions used in this experiment, there is excellent agreement between the calculated and measured values, which is a strong evidence that the measured values are correct. The wavelengths of the manganese lines, together with their designation, are shown in table 1. By using the separation between the first and second manganese lines, the FSR of the Fabry-Pérot etalon was determined to be 18.3989 GHz.

6. Results

Using the methods described in sections 4 and 5, evaluation of the two Doppler shifted thresholds gives the unshifted threshold, i.e. the electron affinity of iodine. The first two rows in table 2 show the Doppler shifted thresholds while the last row shows the value that has been corrected for the Doppler shift.

The conversion from wavelength to electron volts is performed using the new recommended value (Cohen and Taylor 1988) where 1 cm^{-1} equals $1.239\,842\,44\,(37) \times 10^{-4}$ eV. The error of 10 μeV, which corresponds to 2.4 GHz, given in table 2 is the sum of the uncertainties from the determination of the FSR of the Fabry-Pérot etalon and from the threshold determination.

The free spectral range of the Fabry-Pérot is, as mentioned previously, determined by comparing the atomic lines of manganese with the Fabry-Pérot fringes. An error

Table 2. Results of threshold determination.

	E_{Th} (eV)	λ_{Th} (nm)
Threshold parallel beams	3.059 728 (8)	405.2132 (11)
Threshold antiparallel beams	3.058 347 (8)	405.3962 (11)
Threshold unshifted	3.059 038 (10)	405.3047 (13)

in the determination of the FSR of the Fabry-Pérot etalon gives an accumulated error in the measured electron affinity, and this value is estimated to be less than 0.8 GHz. This includes the statistical uncertainty, using two standard deviations, and estimated systematic errors due to the uncertainty of the manganese reference wavelengths and possible shifts in the flame.

The statistical uncertainty obtained in the threshold determination was 1.4 GHz. This includes the statistical uncertainty in both the threshold determination and the determination of the lead line, although the latter is almost negligible (40 MHz). In order to analyse the 1.4 GHz uncertainty obtained in the threshold determination, the different broadening mechanisms which contribute are considered. The total broadening due to the finite interaction time, the divergence of the laser and ion beams and the velocity spread of the ions is approximately 25 MHz. Therefore, the effective bandwidth in this experiment is set only by the frequency width of the laser of 1.2 GHz. This non-zero bandwidth makes the threshold more diffuse and, therefore, more difficult to determine with high accuracy. The non-zero bandwidth also shifts the measured threshold slightly towards lower energies. However, a fit of a theoretical curve which has been convoluted with a 1.2 GHz Gaussian function indicates that this shift is less than 0.2 GHz and well within the uncertainty of the experiment.

As shown in table 2, the threshold wavelength in vacuum is 405.3047 (13) nm, which becomes 405.1902 (13) nm in air. This is in good agreement with the value of Webster *et al* (1983) of 405.18 (2) nm. When this value for the electron affinity is converted to energy units it is 3.059 038 (10) eV, which should be compared with the value of Webster *et al* of 3.0591 (1) eV.

7. Conclusion

We have shown that a pulsed laser, equipped with an intracavity etalon, can be used for high resolution laser photodetachment spectroscopy. Using this technique, we have determined the electron affinity of iodine to be 3.059 038 (10) eV, where the main part of the uncertainty, which is of the order of the laser bandwidth, comes from the statistical uncertainty in the determination of the photodetachment threshold. This can be compared with experiments performed using single mode lasers, for which the best resolution achieved so far is 180 MHz, which is more than two orders of magnitude greater than the laser width. The relatively high resolution achieved using pulsed lasers is a consequence of the high photon flux which, in combination with a gated detection, gives very good counting statistics. Therefore, pulsed lasers are preferable if a resolution of a few GHz is sufficient. When higher resolution is desired, it is necessary to use either a single mode laser or, even better, a single mode laser amplified by a pulsed amplifier, injection seeding, which combines high resolution with high photon flux. Such a system is now under construction in our laboratory and will be used in future experiments.

Acknowledgments

O. Axner and S. Sjöström are gratefully acknowledged for their help with the laser system and with the wavelength calibration measurements. This work was financially supported by the Swedish Natural Science Research Council (NFR).

References

Amusia M Ya, Gribakin G F, Ivanov V K and Chernysheva L V 1990 *J. Phys. B: At. Mol. Opt. Phys.* **23** 385

Axner O, Berglind T, Heully J L, Lindgren I and Rubinsztein-Dunlop H 1984 *J. Appl. Phys.* **55** 3215

Blondel C, Cacciani P, Delsart C and Trainham R 1989a *Phys. Rev.* A **40** 3698

Blondel C, Champeau R-J, Crance M, Crubellier A, Delsart C and Marinescu D 1989b *J. Phys. B: At. Mol. Opt. Phys.* **22** 1335

Blondel C, Champeau R-J, Crubellier A, Delsart C, Duong H T and Marinescu D 1987 *Europhys. Lett.* **4** 1267

Breyer F, Frey P and Hotop H 1978 *Z. Phys.* A **286** 133

Catalán M A, Meggers W F and Garcia-Riquelme O 1964 *J. Res. NBS* A **68** 9

Cohen E R and Taylor B N 1988 *J. Phys. Chem. Ref. Data* **17** 1795

Crance M 1987 *J. Phys. B: At. Mol. Phys.* **20** 6553

—— 1988 *J. Phys. B: At. Mol. Opt. Phys.* **21** 3559

Crosswhite H M 1975 *J. Res. NBS* A **79** 17

Fuller G H 1976 *J. Phys. Chem. Ref. Data* **5** 835

Hall J L, Robinson E J and Branscomb L M 1965 *Phys. Rev. Lett.* **14** 1013

Hanstorp D 1991 The design of an apparatus for photodetachment experiments using collinear laser and ion beams. *In manuscript*

—— 1992 *Meas. Sci. Technol.* **3** 523

Hotop H and Lineberger W C 1985 *J. Phys. Chem. Ref. Data* **14** 731

L'Huillier A and Wendin G 1988 *J. Phys. B: At. Mol. Opt. Phys.* **21** L247

Lineberger W C and Woodward B W 1970 *Phys. Rev. Lett.* **25** 424

Mansour N B, Edge C J and Larson D J 1988 *Nucl. Instrum. Methods* B **31** 313

Neumark D M, Lykke K R, Andersen T and Lineberger W C 1985 *Phys. Rev.* A **32** 1890

Peterson J R, Bae Y K and Huestis D L 1985 *Phys. Rev. Lett.* **55** 692

Radojević V, Kelly H P and Johnson W R 1987 *Phys. Rev.* A **35** 2117

Reader J and Corliss C H 1980 *National Standards Reference Data Series* **68** (Washington, DC: NBS) p 85

Wagenaar H C and de Galan L 1973 *Spectrochim. Acta* B **28** 157

Webster C R, McDermid I S and Rettner C T 1983 *J. Chem. Phys.* **78** 646

Wigner E P 1948 *Phys. Rev.* **73** 1002

Wood D R and Andrew K L 1968 *J. Opt. Soc. Am.* **58** 818